

1 **Distinct signalling routes mediates intercellular and intracellular rhizobial infection**  
2 **in *Lotus japonicus***

3

4 **Short title:** Intercellular infection in *Lotus*

5

6 Jesús Montiel,<sup>a</sup> Dugald Reid,<sup>a</sup> Thomas H. Grønbæk,<sup>a</sup> Caroline M. Benfeldt,<sup>a</sup> Euan K.  
7 James,<sup>b</sup> Thomas Ott,<sup>c</sup> Franck A. Ditengou,<sup>c</sup> Marcin Nadzieja,<sup>a</sup> Simon Kelly,<sup>a,2</sup> and Jens  
8 Stougaard<sup>a,3</sup>

9

10 <sup>a</sup>Department of Molecular Biology and Genetics, Aarhus University, Denmark. DK-8000,  
11 Aarhus C, Denmark

12 <sup>b</sup>The James Hutton Institute, Invergowrie, Dundee, DD2 5DA, United Kingdom

13 <sup>c</sup>Cell Biology, Faculty of Biology, University of Freiburg, 79104 Freiburg, Germany

14

15 Correspondence: Simon Kelly and Jens Stougaard

16 <sup>2</sup>[kelly@mbg.au.dk](mailto:kelly@mbg.au.dk)

17 <sup>3</sup>[stougaard@mbg.au.dk](mailto:stougaard@mbg.au.dk)

18

19 **Contributions**

20 J.M., D.R., C.M.B. and T.H.G. characterised and isolated the mutants. D.R. and J.M.  
21 processed and analysed the RNAseq data, respectively. M.N. and E.K.J. performed the  
22 microscopy analyses. J.M. wrote the manuscript and prepared the figures with contributions  
23 of the co-authors. J.M., S.K. and J.S. conceived the research plan. J.S. and S. K.  
24 coordinated and guided the research.

25 <sup>1</sup>This work was supported by the grant Engineering the Nitrogen Symbiosis for Africa made  
26 to the University of Cambridge by the Bill & Melinda Gates Foundation (ENSA;  
27 OPP11772165). This project has received funding from the European Research Council  
28 (ERC) under the European Union's Horizon 2020 research and innovation programme  
29 (grant agreement No. 834221).

30 **Abstract**

31

32 Rhizobial infection of legume roots during development of nitrogen fixing root  
33 nodules occurs either intracellularly through plant derived infection threads traversing the  
34 epidermal and cortical cell layers to deliver the bacteria or intercellularly via bacterial entry  
35 between epidermal plant cells. Although, around 25% of all legume genera are postulated  
36 to be intercellularly infected, the pathways and mechanisms supporting this process has  
37 remained virtually unexplored due to lack of genetically amenable legumes that have this  
38 infection mode. In this study, we report that the model legume *Lotus japonicus* is infected  
39 intercellularly by *Rhizobium* sp. IRBG74 and demonstrate that the resources available in  
40 *Lotus* enable insight into the genetic requirements and the fine-tuning of the pathway  
41 governing intercellular infection. Inoculation of *Lotus* mutants shows that *Ern1* and *RinRK1*  
42 are dispensable for intercellular infection in contrast to intracellular infection. Other symbiotic  
43 genes, including *Nfr5*, *SymRK*, *CCaMK*, *Epr3*, *Cyclops*, *Nin*, *Nsp1*, *Nsp2*, *Cbs* and *Vpy1* are  
44 equally important for both entry modes. Comparative RNAseq analysis of roots inoculated  
45 with IRBG74 revealed a distinctive transcriptome response compared to intracellular  
46 colonization. In particular, a number of cytokinin-related genes were differentially regulated.  
47 Corroborating this observation *cyp735A* and *ipt4* cytokinin biosynthesis mutants were  
48 significantly affected in their nodulation with IRBG74 while *lhk1* cytokinin receptor mutants  
49 did not form any nodules. These results indicate that a differential requirement for cytokinin  
50 signalling conditions intercellular rhizobial entry and highlight the distinct modalities of the  
51 inter- and intra-cellular infection mechanisms.

52

53

54

55 **Introduction**

56

57 Legumes constitute a large and diverse plant family and most legumes are able to  
58 develop nitrogen fixing root nodules in symbiosis with soil bacteria commonly referred to as  
59 rhizobia. Bacterial infection of roots and root nodules through intracellular infection threads  
60 has been extensively researched in the model legumes *Lotus japonicus* (*Lotus*) and  
61 *Medicago truncatula* (*Medicago*) as well as crop legumes like soybean (*Glycine max* L.), pea  
62 (*Pisum sativum* L.) and common bean (*Phaseolus vulgaris* L.). However, an alternative  
63 mechanism of intercellular infection is widespread in different genera of the Fabaceae family  
64 (Sprent et al., 2017) and suggested to be an ancient and less sophisticated mechanism of  
65 rhizobial colonization (Sprent, 2007). In this process, rhizobia invade the legume roots  
66 between epidermal/root hair cells or by crack entry, during the protrusion of lateral roots  
67 (Coba de la Pena et al., 2017). Intercellular infection processes has been described in detail  
68 by microscopy in different legumes such as *Mimosa*, *Neptunia*, *Stylosanthes*, *Cytisus* and  
69 *Lupinus* (de Faria et al., 1988; James et al., 1992; Subba-Rao et al., 1995; Vega-Hernandez  
70 et al., 2001; Gonzalez-Sama et al., 2004; Goormachtig et al., 2004). Special attention has  
71 been dedicated to characterise the histology of intercellular infection and nodulation  
72 processes in the temperate legumes *Arachis hypogaea*, *Aeschynomene* sp. and the  
73 semiaquatic legume *Sesbania rostrata* (Chandler, 1978; Boogerd and Van Rossum, 1997;  
74 Bonaldi et al., 2011; Ibanez et al., 2017). Under flooded conditions, rhizobial colonization  
75 takes places via infection pockets in *S. rostrata*, formed by a cell death process that depends  
76 on nodulation factors (NFs), perception and localized formation of reactive oxygen species  
77 (D'Haeze et al., 2003). From such infection pockets, cortical infection threads are formed  
78 and migrate to the nodule primordium, where the bacteria are released from the infection  
79 threads (ITs) and colonize the nodule cells in symbiosomes (Capoen et al., 2010). Unlike  
80 intracellular colonization, the leucine-rich repeat-type receptor kinase *SymRK* gene and the  
81 Ca<sup>2+</sup>/calmodulin- dependent protein kinase *CCaMK* gene are dispensable for intercellular  
82 infection in *S. rostrata* by *Azorhizobium caulinodans*. However, these genes are required for  
83 the subsequent intracellular infection threads (Capoen et al., 2005; Capoen et al., 2009). In  
84 peanut (*A. hypogaea*), Bradyrhizobia enter through the middle lamellae of two adjacent root  
85 hairs and spread intercellularly between epidermal and cortical cells. In parallel, adjacent  
86 axillary root hair basal cells become enlarged and infected by the microsymbiont (Chandler,  
87 1978; Boogerd and Van Rossum, 1997; Guha et al., 2016). Both nodule formation and

88 nodule cell colonization require proper exopolysaccharide production by rhizobia (Morgante  
89 et al., 2007). However, invasion and nodule organogenesis can be achieved in peanut by  
90 rhizobia lacking *nod* genes (Ibanez and Fabra, 2011; Guha et al., 2016). Similarly, a NF-  
91 independent nodulation program has been described in certain *Aeschynomene* spp. (Giraud  
92 et al., 2007). Currently, the *A. evenia-Bradyrhizobium* symbiosis has been employed to  
93 study the molecular genetics of this unusual NF-independent symbiosis (Arrighi et al., 2012).  
94 Recent findings show that during this peculiar mechanism, several components of the NF-  
95 dependent process are also recruited, such as SYMRK, CCaMK and the histidine kinase  
96 HK1 cytokinin receptor (Fabre et al., 2015). Additionally, the structural requirements to  
97 perceive NFs in *S. rostrata* are more permissive in intercellular infection compared to the  
98 intracellular infection (Goormachtig et al., 2004). Intercellular infection occurs in several  
99 *Sesbania* spp. by IRBG74 (Cummings et al., 2009), a nodulating *Rhizobium* sp. strain that  
100 is also able to colonize rice and Arabidopsis roots as an endophyte (Biswas et al., 2000;  
101 Mitra et al., 2016; Zhao et al., 2017). Therefore, a better understanding of intercellular  
102 colonization would facilitate the engineering of non-legume crops for colonization by  
103 nitrogen-fixing bacteria.

104 The better characterised intracellular infection is dependent on rhizobial signal  
105 molecules, lipochitooligosaccharides, called nodulation factors (NFs). In *Lotus*, the NFs are  
106 recognized in the plasma membrane of the root hairs by Nod Factor receptors (NFR1, NFR5  
107 and NFR6; (Madsen et al., 2003; Radutoiu et al., 2003; Murakami et al., 2018). A compatible  
108 recognition leads to rhizobial attachment to the root hair tip, promoting its curling to trap the  
109 bacteria with an infection pocket. This give rises to the formation of an infection thread (IT),  
110 a tubular structure with an inward growth that originates from invagination of the plasma  
111 membrane of the root hair. The IT follows a polar growth towards inner root cell layers,  
112 reaching the nodule primordia, formed by the activation of cell division in the cortical cells.  
113 The nodule primordia give rise to a mature nodule, where the bacteria are released from the  
114 IT into symbiosomes and differentiate to become nitrogen-fixing bacteroids (Downie, 2014).

115 The intracellular infection of rhizobia *via* ITs in the root hairs has been extensively  
116 investigated in *Lotus* and *M. truncatula* (Lace and Ott, 2018). In these legumes, the infection  
117 is orchestrated by several transcription factors, including Nodule Inception (*Nin*; (Schäuser  
118 et al., 1999; Marsh et al., 2007) *Nsp1/Nsp2* (Kalo et al., 2005; Heckmann et al., 2006),  
119 *Cyclops* (Yano et al., 2008; Singh et al., 2014) and *ERF* Required for Nodulation (*Ern1*;  
120 (Cerri et al., 2012; Kawaharada et al., 2017). The latter is required for activation of the

121 expression of the cytokinin-biosynthesis genes *Ipt2* and *Log4*, that are major contributors to  
122 the initial cytokinin symbiotic response in *Lotus* (Reid et al., 2017). Cytokinin is necessary  
123 for nodule organogenesis, but plays a negative role during rhizobial invasion. In the cytokinin  
124 oxidase/dehydrogenase 3 mutant (*ckx3*), where cytokinin levels in the roots are increased,  
125 rhizobial infection is significantly reduced (Reid et al., 2016). By contrast, the roots of  
126 cytokinin receptor *Lhk1* mutants are hyperinfected by rhizobia (Murray et al., 2007). Recent  
127 reports show that other receptors have a positive role in infection, like the exopolysaccharide  
128 receptor EPR3 (Kawaharada et al., 2015) and the Leu-rich repeat receptor-like kinase  
129 RINRK1 (Li et al., 2019). In addition, several molecular components are required. Mutants  
130 disrupted in the E3 ligase *Cerberus* (Yano et al., 2009), the nodule pectate lyase *Npl1* (Xie  
131 et al., 2012) or *Arpc1*, *ScarN*, *Nap1*, *Pir1* involved in actin rearrangements (Yokota et al.,  
132 2009; Hossain et al., 2012; Qiu et al., 2015), show defects in IT development and abortion  
133 of the infection process. In *Medicago* the infection thread localized Cystathionine- $\beta$ -  
134 Synthase-like 1 (CBS1; (Sinharoy et al., 2013)), coiled-coil RPG protein (Arrighi et al., 2008)  
135 and Vapyrin (Murray et al., 2011) are crucial components of the root hair infectome (Liu et  
136 al., 2019).

137 In a first step to compare the genetic programs controlling intracellular and  
138 intercellular infection we have explored the infective capacity of *Rhizobium* sp. strain  
139 IRBG74 in *Lotus*, where a wide range of genetic, genomic and transcriptomic resources are  
140 available. Crucial genes for both modalities of rhizobial infection were identified along with  
141 distinctive cellular, transcriptome and genetic requirements for the intercellular colonization.

142

143

144 **Results**

145

146 **IRBG74 induces nitrogen-fixing nodules in *Lotus***

147 The rhizobial strain IRBG74, infects *S. cannabina* intercellularly (Cummings et al.,  
148 2009; Mitra et al., 2016) and interestingly it is also capable of colonizing *O. sativa* and *A.*  
149 *thaliana* roots as an endophyte (Mitra et al., 2016; Zhao et al., 2017). In order to evaluate  
150 the infective capacity of IRBG74 in *Lotus*, nodulation kinetics were recorded from 1 to 6  
151 weeks post-inoculation (wpi) of the Gifu accession. As a control, *L. japonicus* seedlings were  
152 inoculated with its customary symbiont *Mesorhizobium loti* R7A, that infects intracellularly.  
153 Nodule primordia were observed at 1 wpi on *Lotus* roots inoculated with *M. loti*, with mature  
154 pink nodules evident by 2 wpi (Fig. 1A). IRBG74 also induced nodule organogenesis in  
155 *Lotus*, but the first nodule primordia were not observed until 2 wpi (Fig. 1A and B). The first  
156 mature pink nodules on plants inoculated with IRBG74 usually appeared at 3 wpi, but these  
157 were evidently smaller compared to the pink nodules induced by *M. loti* at the same time  
158 point (Fig. 1B). In addition, the number of pink and white nodules were significantly lower at  
159 2 and 3 wpi in plants inoculated with IRBG74 compared to plants inoculated with *M. loti* (Fig.  
160 1A). After 4 to 6 wpi the number of nodules on plants inoculated with *M. loti* and IRBG74  
161 was comparable (Fig. 1A and C). The delay in the IRBG74 nodulation was reflected by the  
162 distribution pattern of the nodules in the root system, since 45% of the nodules were found  
163 in the root crown (upper 2 cm of the root system), while plants inoculated with *M. loti* had  
164 84% of the nodules in this segment of the root (Fig. 1C and D). Nodules induced by IRBG74  
165 were pink and the plant shoots were green (Fig. 1B and C), indicative of nitrogen fixation. At  
166 6 wpi, fresh weight and shoot length were significantly lower, compared to plants inoculated  
167 with *M. loti* reflecting the delayed nodule formation (Fig. 1E and F). These results show that  
168 IRBG74 is able to induce nitrogen-fixing nodules in *Lotus*, albeit with a delay.

169

170 ***Lotus* is intercellularly infected by IRBG74**

171 The delay in organogenesis following inoculation with IRBG74 compared to *M. loti*  
172 prompted us to explore the infection process. For this purpose, the constitutive DsRED  
173 expressing plasmid pSKDSRED was transformed into IRBG74 in order to monitor the early  
174 infection process by confocal microscopy. *M. loti* -DsRed was used as a control. Infection  
175 and nodule organogenesis were unaltered with these engineered strains. Typical

176 intracellular ITs in long root hairs were abundant at 7 dpi with *M. loti* -DsRed (Fig. 2A and  
177 D). In contrast, no IRBG74-DsRed ITs were observed. IRBG74 was attached to the surface  
178 of the roots, mainly associated with the boundaries of the epidermal cells (Fig. 2B). At 2 wpi  
179 IRBG74-DsRed invaded cortical root cell layers intercellularly (Fig. 2C; Supplemental Movie  
180 S1). A detailed and quantitative inspection revealed an average of 35 root hair infection  
181 threads in response to *M. loti*-DsRed, while none were found in the roots inoculated with  
182 IRBG74-DsRed at 10 and 21 dpi (Fig. 2D).

183 In order to characterize the progression of the IRBG74 infection process, the  
184 histology of young and mature nodules was analysed by light microscopy and compared to  
185 nodules of similar developmental stage induced by *M. loti* at 3 wpi. Symbiosome-containing  
186 nodule cells and transcellular ITs were observed in both young and mature nodules of *Lotus*  
187 with both rhizobial strains (Fig. 3A-D; Supplemental Fig. S1). The transcellular ITs were  
188 remarkably more numerous in nodules colonized by *M. loti*, compared to IRBG74,  
189 particularly in young nodules (Fig. 3E).

190

191 ***rinrk1* and *ern1* mutants show contrasting symbiotic phenotypes with IRBG74 and *M.***  
192 ***loti* inoculation**

193 Root infection and nodule organogenesis are highly coordinated multistep processes  
194 and nodule organogenesis is affected in mutants interrupted in rhizobial infection (Oldroyd  
195 and Downie, 2008; Madsen et al., 2010). Nodulation kinetics was therefore a suitable  
196 readout to determine the genetic dependency of the *Lotus*-IRBG74 intercellular process.  
197 IRBG74 and *M. loti* induced nodulation of a set of previously identified *Lotus* symbiotic  
198 mutants was scored at 1-6 wpi. First, mutants affected in the symbiotic receptor genes *Nfr5*,  
199 *SymRK*, *RinRk1* and *Epr3* were tested. Both *M. loti* and IRBG74 were unable to form  
200 nodules in the *nfr5* and *symrk* plants (Supplemental Table S2), indicating that IRBG74  
201 nodulation is Nod factor-dependent and requires functional NF receptors for recognition of  
202 the Nod factor produced by IRBG74 (Crook et al., 2013; Poinsot et al., 2016) to trigger  
203 downstream signal transduction. However, the nodulation performance of the *rinrk1* mutant  
204 was different between plants inoculated with IRBG74 and *M. loti*. In *rinrk1* plants inoculated  
205 with *M. loti* many white uninfected nodules were formed, with very few pink nodules at the  
206 different time points analysed (Fig. 4A and C). In contrast, this hypernodulated-uninfected  
207 phenotype was not observed with IRBG74. The *rinrk1* plants infected by IRBG74 developed

208 similar numbers of nodule structures to w. t. plants inoculated with *M. loti* or IRBG74 at 4-6  
209 wpi, with the majority of them pink, indicating effective rhizobial colonization and symbiosis  
210 (Fig. 4A and F). The number of pink nodules was significantly higher in plants infected by  
211 IRBG74 at 3-6 wpi compared to plants colonized by *M. loti*, indicating that intercellular  
212 infection was not impaired in the *rinrk1* mutant. The role of the expolysaccharide receptor  
213 *EPR3* is apparently important for both types of infection in *L. japonicus*, since a comparable  
214 delayed nodulation phenotype of the *epr3* mutant was observed following inoculation with  
215 *M. loti* or IRBG74 (Fig. S2A).

216 Since the infection process is also controlled by several transcriptional regulators,  
217 the role of *Nin*, *Cyclops*, *Ern1*, *Nsp1* and *Nsp2* were tested with IRBG74. The transcription  
218 factors *Nin*, *Nsp1* and *Nsp2* are indispensable for the symbiotic process established by  
219 IRBG74 and *M. loti*, since the mutants affected in these genes were unable to form nodules  
220 (Supplemental Table S2). The nodulation phenotype of *cyclops* plants inoculated with  
221 IRBG74 and *M. loti* was similar, and only uninfected white nodules developed (Supplemental  
222 Fig. S2B). However, a clear difference was found in the symbiotic performance of the *ern1*  
223 mutant. The first pink nodules appeared at 4 wpi with *M. loti* (Fig. 4A and D), while in the  
224 presence of IRBG74 these were detected at 3 wpi with fully developed pink nodules at 4 wpi  
225 (Fig. 4A, G). This is the reverse of the kinetics shown by w. t. plants wherein pink nodules  
226 emerged at 2 and 3 wpi with *M. loti* and IRBG74, respectively (Fig. 1A and B). Additionally,  
227 both the total number of nodules and pink nodules was higher in *ern1* mutants with IRBG74  
228 at 3-6 wpi, compared to *M. loti* (Fig. 4A).

229

230

### 231 **Nodulation by IRBG74 is negatively impacted in root hair IT mutants**

232 In *Lotus* several genes participating in a wide variety of molecular processes have  
233 been described as important for IT progression. For instance, the *Lotus* mutants affected in  
234 the U-box protein *Cerberus* (Yano et al., 2009), the nodule pectate lyase *Npl1* (Xie et al.,  
235 2012) or the cytoskeleton component *ScarN* (Qiu et al., 2015), show defects in IT growth  
236 and progression. The contribution of these genes to the intercellular infection of IRBG74  
237 was therefore assessed. These mutants were characterized by the formation of a high  
238 proportion of white nodules both with *M. loti* and IRBG74 (Supplemental Fig. S2C-E), and  
239 few pink nodules were developed in the *npl1* and *scarN* mutants (Supplemental Fig. S2D

240 and E). In all these mutants, the number of nodule structures was reduced when IRBG74  
241 was used as inoculum (Supplemental Fig. S2C-E).

242 In *Medicago* IT development has been shown to require the function of the *Vapyrin*,  
243 *RPG* and *Cbs* genes. Since the participation of these genes has not been reported in *Lotus*-  
244 rhizobia symbiosis, their homolog counterparts were identified in the *Lotus* genome  
245 (<https://lotus.au.dk/>). For *Vapyrin*, two homologous genes named *LjVpy1*  
246 (LotjaGi2g1v0091200) and *LjVpy2* (LotjaGi1g1v0646300) (Supplemental Table S1)  
247 encoding proteins with 77% and 69% identity to the *MtVPY* protein, respectively. Similarly,  
248 two genes encoding proteins with 61% and 31% amino acid identities to *MtRPG* were named  
249 *LjRPG* (LotjaGi5g1v0253300) and *LjRPG-like* (LotjaGi5g1v0086600), respectively  
250 (Supplemental Table S1). The *LjCBS* found (LotjaGi2g1v0126500) showed 78% of protein  
251 similarity to *MtCBS*. Using the LORE1 database, mutant lines with LORE1 insertions were  
252 identified and genotyped to obtain homozygous mutant plants. A delay in nodule  
253 organogenesis was observed for all the mutants inoculated with *M. loti*, reflected by a  
254 reduced number of nodules within the first week after rhizobial inoculation (Supplemental  
255 Fig. S2F-J). In response to IRBG74 inoculation, nodulation was also delayed in *vpy1* and  
256 *vpy2* (Supplemental Fig. S2G and H), but not in the *rpg* and *rpg-l* mutants, where the number  
257 of nodules were similar to the w. t. plants at different time points (Supplemental Fig. S2I and  
258 J). Based on the nodule numbers, *vpy1* plants were more severely impacted with IRBG74  
259 (Supplemental Fig. S2G), while the *vpy2* mutant was more affected with *M. loti*  
260 (Supplemental Fig S4H). However, at 5 and 6 wpi both the total number of nodules and pink  
261 nodules, tended to be similar between the w. t. and mutants. Since *MtVpy* and *MtRPG* have  
262 been described as important for IT development in *Medicago*, the number of root hair ITs  
263 was recorded in mutants affected in these genes in *Lotus* at 1 wpi with *M. loti*-DsRed. A  
264 significant reduction of IT numbers of around 50% in the *vpy1*, *vpy2* and *rpg* mutants  
265 compared to w. t. was observed (Supplemental Table S3).

266

## 267 **Disposable role of ROS and ethylene in the *Lotus*-IRBG74 symbiosis**

268 It has been described that ethylene plays a positive role in the intercellular infection  
269 and nodulation program in the *S. rostrata*-*Azorhizobium* symbiosis (D'Haeze et al., 2003).  
270 To determine the role of this phytohormone in the *Lotus*-IRBG74 symbiotic process, the  
271 nodulation kinetics of the double mutant insensitive to ethylene *ein2a ein2b* (Reid et al.,

272 2018) was recorded. The first nodule structures appeared at 2 wpi in the *ein2a ein2b* mutant  
273 inoculated with IRBG74, showing a hypernodulation phenotype in the subsequent weeks.  
274 However, the total number of nodules induced by IRBG74 was considerably lower than *M.*  
275 *loti* (Supplemental Fig. S2K). In addition, ethylene production was lower in w. t. *Lotus* roots  
276 inoculated with IRBG74 in comparison to plants treated with *M. loti* (Supplemental Fig. S3).  
277 Taken together, these results show that ethylene is not playing a pivotal role in the infection  
278 and organogenesis program triggered by IRBG74 in *Lotus*.

279 In several legumes it has been shown that reactive oxygen species (ROS) produced  
280 by respiratory burst oxidase homolog (RBOH) enzymes are required for intracellular and  
281 intercellular infection (Peleg-Grossman et al., 2007; Montiel et al., 2012; Montiel et al., 2016;  
282 Arthikala et al., 2017). To address the involvement of these compounds in the symbiotic  
283 process induced by IRBG74 in *Lotus*, homozygous mutant lines affected in two *Rboh*  
284 isoforms, *LjRbohE* (LotjaGi5g1v0224200) and *LjRbohG* (LotjaGi1g1v0771200), were  
285 obtained from the LORE1 database. *LjRbohE* and *LjRbohG* are putative orthologs of  
286 *MtRbohA* and *PvRbohB*, previously characterised genes, required for nodule functioning  
287 and rhizobial infection in *Medicago* and common bean, respectively (Marino et al., 2011;  
288 Montiel et al., 2012). In response to *M. loti* inoculation both *rbohE* and *rbohG* showed a  
289 reduced number of nodule primordia and pink nodules at 1 wpi (Supplemental Fig. S2L and  
290 M). However, in the ensuing weeks these nodule structures attained similar numbers to w.  
291 t. plants at all timepoints tested. The nodulation kinetics of these *rboh* mutants in response  
292 to IRBG74 infection was comparable to the w. t. plants (Supplemental Fig. S2L and M),  
293 which indicate that these genes are not playing an important role in the intercellular  
294 colonization by IRBG74 in *Lotus*.

295

## 296 **Intercellular infection by IRBG74 promotes a distinct transcriptional reprogramming**

297 The nodulation assays of the *Lotus* mutants inoculated with IRBG74 showed that the  
298 genetic dependencies for intercellular and intracellular infection modes differ. To further  
299 evaluate the signalling pathways involved in intercellular infection, RNAseq transcriptome  
300 data were collected and analysed from IRBG74-inoculated *Lotus* roots at 3, 5 and 10 dpi, to  
301 cover the infection phase preceding nodule organogenesis. These data were compared to  
302 available RNAseq information on *Lotus* roots harvested at 1 and 3 dpi with *M. loti* (Mun et  
303 al., 2016; Kamal et al., 2020). In response to *M. loti* and IRBG74 inoculation, a total of 12,637

304 and 10,947 differentially expressed genes (DEG, P-adjust < 0.5) were identified,  
305 respectively (Supplemental Fig. S4A; Supplemental Table S4). The largest transcriptome  
306 responses were observed at 1 dpi with *M. loti* (12,534) and at 10 dpi with IRBG74 (9,438)  
307 DEG (Supplemental Fig. S4B). A more stringent analysis, with the DEG showing a LOG2FC  
308  $\geq 2$ , revealed that the most important transcriptome response was triggered at 5 dpi IRBG74  
309 (Fig. 5A). Interestingly, only 33% of the DEG by *M. loti* were similarly affected by IRBG74  
310 and a large proportion of the up/down-regulated genes during *M. loti* infection (314: sum of  
311 the up and down-regulated) were not similarly affected by IRBG74 (Fig. 5B and C).  
312 Additionally, the majority of the genes down-regulated in response to IRBG74 inoculation  
313 were not repressed in the *M. loti* transcriptome (Fig. 5B and C).

314 The nodulation kinetics of *Lotus* inoculated with IRBG74 revealed that nodule  
315 organogenesis was delayed with respect to plants inoculated with *M. loti*. To determine if  
316 this delay was linked to a deficient induction of the early symbiotic signalling pathway, the  
317 expression profile of several genes known to be involved in infection and/or nodule  
318 organogenesis were analysed using the transcriptome data set. Most of the known symbiotic  
319 genes tested were induced by *M. loti* or IRBG74 (Fig. 5D), but when the same time point  
320 was compared (3 dpi), several genes were less upregulated in response to IRBG74  
321 inoculation (Fig. 5D).

322

### 323 **Cytokinin signalling is differentially regulated in response to IRBG74**

324 This work showed that *Ern1*, a transcription factor implicated in cytokinin signalling  
325 (Cerri et al., 2017; Kawaharada et al., 2017), has a less relevant role during intercellular  
326 infection by IRBG74. These results suggest that this mode of infection triggers a different  
327 transcriptional response of cytokinin-related genes compared to intracellular infection. To  
328 validate this hypothesis, a transcriptome heat-map was created for genes involved in  
329 cytokinin synthesis and regulation and significantly affected by *M. loti* or IRBG74 inoculation  
330 (Fig. 6). This approach confirmed the different gene-expression response of several  
331 components of cytokinin regulation during IRBG74 infection. Particularly, genes encoding  
332 the cytokinin degrading enzymes *Ckx3*, *Ckx9*, the response regulator involved in cytokinin  
333 signalling *RR11a* and the cytokinin biosynthesis gene *Ipt2* were poorly or insignificantly  
334 induced during intercellular infection, relative to their evident up-regulation after *M. loti*  
335 inoculation (Fig. 6). *M. loti* triggered a significant reduction in the expression levels of *Ckx2*,

336 *Ckx8*, *Lhk2*, *RR3a*, *RR19*, and *Log*. However, most of these genes were not significantly  
337 down-regulated by IRBG74 colonization. By contrast, the cytokinin biosynthesis gene  
338 *Cyp735a*, which converts iP to tZ type cytokinins, showed a strong up-regulation after  
339 IRBG74 colonization at 5 and 10 dpi, whereas its gene expression was only slightly altered  
340 during intracellular infection at early timepoints (Fig. 6).

341

342 ***Cyp735a*, *Ipt4* and *Lhk1* are relevant players in the *Lotus*-IRBG74 symbiosis**

343 In the *Lotus*-*M. loti* symbiosis, the cytokinin receptor mutant *lhk1* shows a delayed  
344 and reduced nodulation (Murray et al., 2007), while the *ipt4* and *cyp735a* mutants show  
345 minor or insignificant phenotypes, respectively (Reid et al., 2017; Supplemental Fig. S5).  
346 The RNAseq data presented in this study indicates that these genes are differentially  
347 regulated by *M. loti* or IRBG74. In order to determine the relevance of these cytokinin-related  
348 genes in the *Lotus*-IRBG74 symbiosis, nodulation kinetics at 1-6 wpi were scored for the  
349 *cyp735a*, *ipt4* and *lhk1* mutants after IRBG74 inoculation. The nodulation capacity of both  
350 *cyp735a* and *ipt4* mutants was substantially reduced, although with different symbiotic  
351 phenotypes. The *cyp735a* mutant developed similar numbers of nodules to w. t. plants, at 2  
352 and 3 wpi (Fig. 7A), but at 4-6 wpi *cyp735a* formed more nodule-like structures, most of  
353 them uninfected white nodules (Fig 7C, right panel). By contrast, at 2-4 wpi the total number  
354 of nodules in *ipt4* was lower compared to w. t. plants (Fig. 7A). The number of pink nodules  
355 was reduced at all time points tested and these comprised a mixture of pink and pale pink  
356 nodules (Fig. 7A and D, right panel). Interestingly the *lhk1* mutant was unable to develop  
357 any nodule structure in the presence of IRBG74 (Fig. 7A). This drastic symbiotic phenotype  
358 contrasts with the *lhk1* plants inoculated with *M. loti*, where several pink nodules were  
359 observed at 6 wpi (Supplemental Fig. S6). These results further demonstrate the different  
360 cytokinin regulation during intercellular infection in *Lotus*, whereby *Cyp735a*, *Ipt4* and *Lhk1*  
361 are important players for this type of rhizobial infection (Fig. 8).

362

363 **Discussion**

364

365 ***Lotus*-IRBG74 symbiosis: a novel working model to study intercellular infection**

366            Intercellular colonization of legumes by rhizobia occurs via a variety of entry modes.  
367            Bacteria can penetrate through middle lamellae of root hairs, cracks at emergent lateral  
368            roots or between epidermal cells (Subba-Rao et al., 1995; Gonzalez-Sama et al., 2004;  
369            Goormachtig et al., 2004; Bonaldi et al., 2011). Diverse *Lotus* spp. exhibit this infection  
370            mechanism, which leads to the formation of either ineffective or nitrogen-fixing nodules,  
371            depending on the growth conditions and rhizobial partner (Ranga Rao, 1977; James and  
372            Sprent, 1999; Liang et al., 2019). Previously, it was described that under certain mutant  
373            background conditions and with a low frequency, *Lotus* roots can be intercellularly colonized  
374            by *M. loti* (Madsen et al., 2010) by a NF-independent mechanism. Here we show that  
375            IRBG74 massively accumulates on the root surface of *Lotus* roots and invades the roots  
376            between the epidermal and root hair cells. This intercellular invasion transforms into  
377            transcellular infection threads in inner root cell layers and the nodule. A similar scenario has  
378            been described in *S. rostrata*, where the infection pocket, formed by an intercellular invasion  
379            of certain *Azorhizobium* spp., is followed by transcellular infection threads (Goormachtig et  
380            al., 2004). Although IRBG74 promoted nodule formation in *Lotus*, the organogenesis and  
381            infection programs were delayed, compared to the symbiotic proficiency of *M. loti*. This delay  
382            is apparently not related to the infection mode, since the infection and nodule organogenesis  
383            program in *A. hypogaea*, which is also intercellularly invaded, exhibit comparable kinetics to  
384            those observed in the model legumes *Lotus* or *Medicago*, wherein root hair ITs are formed.

385

### 386            **Common gene dependencies of intercellular and intracellular colonization**

387            The characterisation of several legume mutants has identified the molecular players  
388            of the symbiotic pathway, from the early signalling to nodule organogenesis. NF receptors  
389            are indispensable for initiating symbiotic signalling, since *Lotus* mutants disrupted in these  
390            genes do not show any symbiotic response (Madsen et al., 2003; Radutoiu et al., 2003).  
391            The nodulation test of *Ljnfr5* with IRBG74 revealed that functional NF receptors are required  
392            for the *Lotus*-IRBG74 symbiosis. Likewise, both intercellular rhizobial infection and nodule  
393            organogenesis is a NF-dependent process in the *S. rostrata*-*A. caulinodans* relationship  
394            (Capoen et al., 2010), but there are also intercellular processes whereby a NF-independent  
395            mechanism can lead to nitrogen-fixing nodules in certain legumes (Giraud et al., 2007;  
396            Madsen et al., 2010; Ibanez and Fabra, 2011). This study revealed a genetic machinery that  
397            is equally important for both types of infection modes, since a similar detrimental impact in  
398            the nodulation process was observed in the *nfr5*, *symrk*, *ccamk*, *cyclops*, *nin*, *nsp1*, *nsp2*

399 *epr3*, *cbs* and *vpy1* mutants whether *M. loti* or IRBG74 were used as inoculum in *Lotus* (Fig.  
400 8). However, the intracellular symbiotic program was more affected in the *rinrk1*, *ern1*,  
401 *rbohE*, *rbohG*, *rpg*, *rpg-like*, and *vpy2* mutants. One interpretation is that these genes are  
402 more important for formation of root hair ITs than transcellular ITs. Previously, it was  
403 described in *A. evenia* that SYMRK, CCaMK and the histidine kinase HK1 are required both  
404 in the intracellular and intercellular infection by *Bradyrhizobium* (Fabre et al., 2015),  
405 reinforcing the notion of a common genetic repertoire for these types of rhizobial infection.  
406 Likewise, SYMRK and CCaMK are required for intercellular infection and nodulation in the  
407 IRBG74-*Lotus* symbiosis. However, the symbiotic process through intercellular colonization  
408 is apparently more sensitive to the absence of certain genes. *cerberus*, *npl1* and *scarN*  
409 mutants developed numerous white nodules, frequently uninfected after *M. loti* inoculation  
410 (Yano et al., 2009; Xie et al., 2012; Qiu et al., 2015), but when IRBG74 was used as  
411 inoculum, nodule development and the number of pink nodules were severely reduced in  
412 these mutants. This suggests that actin rearrangement play an important role in formation  
413 of cortical and transcellular infection threads and that initiation of ITs from intercellular  
414 infection pockets is more dependent on actin rearrangement.

415 As mentioned above, there are few reports describing the molecular components  
416 required for intercellular infection. One of them, revealed the positive role of ROS to induce  
417 cell death during the crack entry infection of *Azorhizobium* in *S. rostrata*. Deprivation of ROS  
418 production by applying diphenyleneiodonium chloride, an inhibitor of the ROS-producing  
419 enzymes RBOHs (for respiratory burst oxidase homolog), prevents rhizobial colonization in  
420 this legume (D'Haeze et al., 2003). Similarly, these genes have been implicated in the IT  
421 development during intracellular rhizobial infection in *Medicago* and *P. vulgaris* (Peleg-  
422 Grossman et al., 2007; Montiel et al., 2012; Arthikala et al., 2017). Likewise, the nodulation  
423 program was delayed in *Lotus* mutants disrupted in *RbohE* or *RbohG* genes after inoculation  
424 with *M. loti*, however, the nodulation kinetics in these mutants was unchanged by IRBG74.  
425 Inhibition of ethylene synthesis or perception has a negative effect in the nodulation and  
426 intercellular infection induced by *Azorhizobium* in *S. rostrata* (D'Haeze et al., 2003). In  
427 contrast, ethylene plays a negative role in the *Lotus*-*M. loti* symbiosis. The *Ljein2a* *Ljein2b*  
428 double mutant that exhibits complete ethylene insensitivity is hyperinfected and  
429 hypernodulated by *M. loti* (Reid et al., 2018). Unlike, the intercellular symbiotic process in *S.*  
430 *rostrata*, where ethylene is required for nodulation, the *Ljein2a* *Ljein2b* mutant was  
431 hypernodulated by IRBG74, indicating that this phytohormone is not essential for the IRBG74  
432 intercellular infection.

433

434 **Distinctive cytokinin signalling program during intercellular infection**

435 The dual role of cytokinins, as positive and negative regulators of nodule  
436 development and rhizobial infection, respectively, makes them key phytohormones in the  
437 legume-rhizobia symbiosis (Miri et al., 2016). The *lhk1* mutant belatedly develops a reduced  
438 number of pink nodules in response to *M. loti* infection, but when IRBG74 is used as  
439 inoculum the mutant is unable to form nodules up to 6 wpi. In the intracellular infection  
440 mediated by *M. loti*, it has been suggested that other cytokinin receptors are sufficient to  
441 induce nodule organogenesis in the absence of *Lhk1* (Murray et al., 2007). However, the  
442 signalling pathway triggered by LHK1 is indispensable in the *Lotus*-IRBG74 symbiosis.  
443 Conversely, the *ern1* mutant displayed improved symbiotic performance with IRBG74, which  
444 further confirms that depending on the type of rhizobial infection program, distinct signalling  
445 pathways are triggered. This was reflected in the different transcriptomic responses of genes  
446 involved in the synthesis, perception signalling and metabolism of cytokinin induced by *M.*  
447 *loti* or IRBG74. Similarly, the *A. hypogaea* roots intercellularly infected by rhizobia, exhibit a  
448 distinctive transcriptome profile of genes involved in cytokinin metabolism and signalling,  
449 when compared to the expression pattern of orthologue genes in legumes intracellularly  
450 colonized (Peng et al., 2017; Karmakar et al., 2019). It has been shown that different  
451 cytokinin biosynthesis genes are induced during intracellular colonization of *M. loti* in *Lotus*  
452 roots (Reid et al., 2016; Reid et al., 2017). Although the cytokinin *trans*-hydroxylase  
453 *Cyp735a* is highly induced by *M. loti*, the nodulation performance is not significantly affected  
454 in *Lotus* plants disrupted in this gene (Reid et al., 2017). By contrast, nodule organogenesis  
455 is delayed and reduced in *cyp735a* mutants inoculated with IRBG74. *Cyp735a* encodes  
456 cytochrome P450 monooxygenases (P450s) that catalyze the biosynthesis of trans-Zeatin,  
457 an isoprenoid cytokinin compound (Takei et al., 2004), indicating that tZ cytokinins play a  
458 more relevant role during intercellular colonization. The mutant affected in the isopentenyl  
459 transferase 4 (*Ipt4*) gene, showed a mild impact in the nodulation capacity with *M. loti* (Reid  
460 et al., 2017). However, in response to IRBG74 inoculation, the development of nodules was  
461 evidently delayed, and the number of pink nodules reduced. IPT is placed in the first step  
462 during isoprenoid cytokinin biosynthesis, giving rise to iP riboside 50 -diphosphate (iPRDP)  
463 or iP riboside 50 - triphosphate (iPRTP) intermediates, which can be converted by CYP735a  
464 to tZ cytokinins (Hwang and Sakakibara, 2006). The delayed nodulation and enhanced  
465 phenotypes of the cytokinin related mutants may indicate that the peak of cytokinin triggered

466 by the intercellular programme is lower or more disperse in the root relative to the highly  
467 localised cytokinin signalling achieved in the intracellular infection modes.

468

## 469 **Conclusions**

470

471 The intracellular colonization has been extensively described at the cellular level in  
472 recent decades, but there is little knowledge about the molecular players controlling the  
473 intercellular invasion. Different approaches revealed that the cytokinin signalling pathway is  
474 apparently a key difference to be further analysed. Similarly, other components seem to be  
475 differentially relevant for this type of infection. For instance, the *rinrk1* receptor mutant  
476 showed a better nodulation performance with IRBG74 compared to *M. loti*. This latter  
477 indicates that during intercellular infection, certain uncharacterized ligands are not entirely  
478 necessary for rhizobial colonization.

479

## 480 **Material and Methods**

481

### 482 **Germination and Nodulation assays**

483 *Lotus* seeds of accession Gifu (Handberg and Stougaard, 1992) were scarified with  
484 sandpaper were surface sterilized with 0.3% of sodium hypochlorite for 10 minutes and then  
485 washed 5 times with autoclaved distilled water, to remove traces of chlorine. The washed  
486 seeds were incubated overnight at 4 °C and then transferred to square petri dishes for  
487 germination at 21 °C. For monitoring nodulation kinetics, three days post-germination  
488 seedlings ( $n \geq 20$  plants per condition) were placed into petri dishes with 1.4% B&D agar  
489 slant covered with filter paper and inoculated with the respective rhizobial strains ( $OD_{600} =$   
490 0.05). After rhizobial inoculation the number of white (bumps and nodule primordia) and pink  
491 nodules were recorded weekly until 6 weeks post inoculation (wpi) with a stereomicroscope.  
492 The plants were harvested at 6 wpi to measure the fresh weight and length of the aerial part.  
493 LORE1 lines (Urbanski et al., 2012; Malolepszy et al., 2016) disrupted in the genes of  
494 interest were ordered from the LORE1 database (<https://lotus.au.dk/>) and genotyped with  
495 allele-specific primers to obtain homozygous mutants following the database instructions

496 (Mun et al., 2016). The gene IDs and the corresponding LORE1 IDs are shown in  
497 Supplemental Table S1.

498

#### 499 **Infection phenotyping using confocal microscopy**

500 Three days old seedlings of *Lotus* (accession Gifu) (Handberg and Stougaard, 1992)  
501 were placed on ¼ B&D plates and inoculated with fluorescently labelled *M. loti* R7A (Kelly  
502 et al., 2013) or IRBG74 strains (Cummings et al., 2009), obtained through transformation  
503 with the constitutive DsRED expressing plasmid pSKDSRED (Kelly et al., 2013). The roots  
504 were harvested from the plates at different time points. To enable observations in deeper  
505 part of the tissue, fluorescent compatible clearing protocol was used as described before  
506 (Nadzieja et al., 2019). Cleared roots were visualized by confocal microscopy with the  
507 following excitation lasers/emission cutoffs: 405/408–498 nm (autofluorescence), 561/517–  
508 635 nm (DsRed). For 3D projections, Fiji ImageJ (Schindelin et al., 2012) was used to create  
509 animation frames, which then were rearranged using Adobe Photoshop CC into final  
510 projections.

511

#### 512 **Nodule histology analysis**

513 Young and mature nodules at 3 wpi with IRBG74 or *M. loti* were detached from *Lotus*  
514 roots, sliced in half, and incubated overnight in fixative solution (2.5% glutaraldehyde, 0.1 M  
515 sodium cacodylate pH 7). The fixed nodules slices were embedded in acrylic resin and  
516 sectioned for light microscopy (James and Sprent, 1999; Madsen et al., 2010).

517

#### 518 **RNAseq of *Lotus* roots and bioinformatics**

519 The susceptible infection zone of *L. japonicus* roots by IRBG74 (elongation and  
520 maturation zone of the root) was cut and freeze in liquid nitrogen from seedlings at 3, 5 and  
521 10 dpi with IRBG74 (O. D. 600 = .05) or mock-treated (water) at the same time points.  
522 Total RNA was isolated and DNA contamination was removed by DNase treatment. Library  
523 preparations using randomly fragmented mRNA was performed by IMGM laboratories  
524 (Martinsried, Germany) and sequenced in paired-end 150 bp mode on a Illumina NovaSeq  
525 6000 instrument.

526 A decoy-aware index was built for Gifu transcripts using default Salmon parameters and  
527 reads were quantified using the --validateMappings flag (Salmon version 0.14.1; Patro et  
528 al., 2017). Normalised expression levels and differential expression testing was performed  
529 using the R-package DESeq2 version 1.20 (Love et al., 2014) after summarising gene level  
530 abundance using the R-package tximport (version 1.8.0).

531

532 **Accession numbers**

533 The RNAseq reads associated with this study are available in the SRA under  
534 bioproject accession number PRJNA632725. The *L. japonicus* (accession Gifu and MG20)  
535 gene identifiers are shown in Supplemental Table S1.

536

537 **Large datasets**

538 The calculated expression values and statistics of the RNAseq data are included as  
539 Supplemental Table S4.

540

541 **Acknowledgements**

542 We thank the assistance in the greenhouse of Finn Pedersen and Nanna Walther.  
543 We thank Dr. Fang Xie for providing *rinrk1* seeds.

544

545 **Supplemental Material**

546 Supplemental Figure S1. Nodule cell occupancy in *Lotus* nodules colonized by *M. loti* or  
547 IRBG74.

548 Supplemental Figure S2. Nodulation performance of *Lotus* mutants.

549 Supplemental Figure S3. Ethylene production in *Lotus* roots inoculated with rhizobia.

550 Supplemental Figure S4. DEG in *Lotus* roots after rhizobial inoculation.

551 Supplemental Figure S5. Phenotype of *cyp735a* and *ipt4* mutants inoculated with *M. loti*.

552 Supplemental Figure S6. Phenotype of *lhk1* plants inoculated with *M. loti* or IRBG74.

- 553 Supplemental Table S1. List of *Lotus* mutants used in this study.
- 554 Supplemental Table S2. *Lotus* mutants with a Nod- phenotype in response to *M. loti* or
- 555 IRBG74 inoculation.
- 556 Supplemental Table S3. Number of ITs per plant at 1 wpi with *M. loti*.
- 557 Supplemental Table S4. RNAseq expression data of *Lotus* roots inoculated with *M. loti* (1
- 558 and 3 dpi) or IRBG74 (3, 5 and 10 dpi).
- 559 Supplemental Video S1. 3D-projection of *Lotus* roots infected by IRBG74 at 1 and 2 wpi.
- 560

561 **References**

- 562
- 563 **Arrighi JF, Cartieaux F, Brown SC, Rodier-Goud M, Boursot M, Fardoux J, Patrel D, Gully D, Fabre**  
564 **S, Chaintreuil C, Giraud E** (2012) *Aeschynomene evenia*, a model plant for studying the  
565 molecular genetics of the nod-independent rhizobium-legume symbiosis. *Mol Plant*  
566 *Microbe Interact* **25**: 851-861
- 567 **Arrighi JF, Godfroy O, de Billy F, Saurat O, Jauneau A, Gough C** (2008) The RPG gene of *Medicago*  
568 *truncatula* controls Rhizobium-directed polar growth during infection. *Proc Natl Acad Sci U*  
569 *S A* **105**: 9817-9822
- 570 **Arthikala MK, Montiel J, Sanchez-Lopez R, Nava N, Cardenas L, Quinto C** (2017) Respiratory Burst  
571 Oxidase Homolog Gene A Is Crucial for Rhizobium Infection and Nodule Maturation and  
572 Function in Common Bean. *Front Plant Sci* **8**: 2003
- 573 **Biswas JB, Ladha JK, Dazzo FB, Yanni YG, Rolfe BG** (2000) Rhizobial Inoculation Influences Seedling  
574 Vigor and Yield of Rice. *Agron J* **92**: 880-886
- 575 **Bonaldi K, Gargani D, Prin Y, Fardoux J, Gully D, Nouwen N, Goormachtig S, Giraud E** (2011)  
576 Nodulation of *Aeschynomene aeraspera* and *A. indica* by photosynthetic Bradyrhizobium Sp.  
577 strain ORS285: the nod-dependent versus the nod-independent symbiotic interaction. *Mol*  
578 *Plant Microbe Interact* **24**: 1359-1371
- 579 **Boogerd FC, Van Rossum D** (1997) Nodulation of groundnut by Bradyrhizobium: a simple infection  
580 process by crack entry. *FEMS Microbiol. Rev.* **21**: 5-7
- 581 **Capoen W, Den Herder J, Sun J, Verplancke C, De Keyser A, De Rycke R, Goormachtig S, Oldroyd**  
582 **G, Holsters M** (2009) Calcium spiking patterns and the role of the calcium/calmodulin-  
583 dependent kinase CCaMK in lateral root base nodulation of *Sesbania rostrata*. *Plant Cell* **21**:  
584 1526-1540
- 585 **Capoen W, Goormachtig S, De Rycke R, Schroevers K, Holsters M** (2005) SrSymRK, a plant receptor  
586 essential for symbiosome formation. *Proc Natl Acad Sci U S A* **102**: 10369-10374
- 587 **Capoen W, Oldroyd G, Goormachtig S, Holsters M** (2010) *Sesbania rostrata*: a case study of natural  
588 variation in legume nodulation. *New Phytol* **186**: 340-345
- 589 **Cerri MR, Frances L, Laloum T, Auriac MC, Niebel A, Oldroyd GE, Barker DG, Fournier J, de**  
590 **Carvalho-Niebel F** (2012) *Medicago truncatula* ERN transcription factors: regulatory

- 591 interplay with NSP1/NSP2 GRAS factors and expression dynamics throughout rhizobial  
592 infection. *Plant Physiol* **160**: 2155-2172

593 **Cerri MR, Wang Q, Stolz P, Folgmann J, Frances L, Katzer K, Li X, Heckmann AB, Wang TL, Downie**  
594 **JA, Klingl A, de Carvalho-Niebel F, Xie F, Parniske M** (2017) The ERN1 transcription factor  
595 gene is a target of the CCaMK/CYCLOPS complex and controls rhizobial infection in *Lotus*  
596 *japonicus*. *New Phytol* **215**: 323-337

597 **Coba de la Pena T, Fedorova E, Pueyo JJ, Lucas MM** (2017) The Symbiosome: Legume and Rhizobia  
598 Co-evolution toward a Nitrogen-Fixing Organelle? *Front Plant Sci* **8**: 2229

599 **Crook MB, Mitra S, Ane JM, Sadowsky MJ, Gyaneshwar P** (2013) Complete Genome Sequence of  
600 the *Sesbania* Symbiont and Rice Growth-Promoting Endophyte *Rhizobium* sp. Strain IRBG74.  
601 *Genome Announc* **1**

602 **Cummings SP, Gyaneshwar P, Vinuesa P, Farruggia FT, Andrews M, Humphry D, Elliott GN, Nelson**  
603 **A, Orr C, Pettitt D, Shah GR, Santos SR, Krishnan HB, Odee D, Moreira FM, Sprent JI, Young**  
604 **JP, James EK** (2009) Nodulation of *Sesbania* species by *Rhizobium* (*Agrobacterium*) strain  
605 IRBG74 and other rhizobia. *Environ Microbiol* **11**: 2510-2525

606 **Chandler MR** (1978) Some observations on infection of *Arachis hypogaea* L. by rhizobium. *J Exp Bot*  
607 **29**: 749-755

608 **D'Haeze W, De Rycke R, Mathis R, Goormachtig S, Pagnotta S, Verplancke C, Capoen W, Holsters**  
609 **M** (2003) Reactive oxygen species and ethylene play a positive role in lateral root base  
610 nodulation of a semiaquatic legume. *Proc Natl Acad Sci U S A* **100**: 11789-11794

611 **de Faria S, Hay G, Sprent JI** (1988) Entry of rhizobia into roots of *Mimosa scabrella* Bentham occurs  
612 between epidermal cells. *Journal of General Microbiology* **134**: 2291-2296

613 **Downie JA** (2014) Legume nodulation. *Curr Biol* **24**: R184-190

614 **Fabre S, Gully D, Poitout A, Patrel D, Arrighi JF, Giraud E, Czernic P, Cartieaux F** (2015) Nod Factor-  
615 Independent Nodulation in *Aeschynomene evenia* Required the Common Plant-Microbe  
616 Symbiotic Toolkit. *Plant Physiol* **169**: 2654-2664

617 **Giraud E, Moulin L, Vallenet D, Barbe V, Cytryn E, Avarre JC, Jaubert M, Simon D, Cartieaux F, Prin**  
618 **Y, Bena G, Hannibal L, Fardoux J, Kojadinovic M, Vuillet L, Lajus A, Cruveiller S, Rouy Z,**  
619 **Mangenot S, Segurens B, Dossat C, Franck WL, Chang WS, Saunders E, Bruce D, Richardson**  
620 **P, Normand P, Dreyfus B, Pignol D, Stacey G, Emerich D, Vermeglio A, Medigue C,**  
621 **Sadowsky M** (2007) Legumes symbioses: absence of Nod genes in photosynthetic  
622 bradyrhizobia. *Science* **316**: 1307-1312

623 **Gonzalez-Sama A, Mercedes-Lucas MM, De Felipe MR, Pueyo JJ** (2004) An unusual infection  
624 mechanism and nodule morphogenesis in white lupin (*Lupinus albus*). *New Phytol* **163**: 371-  
625 380

626 **Goormachtig S, Capoen W, James EK, Holsters M** (2004) Switch from intracellular to intercellular  
627 invasion during water stress-tolerant legume nodulation. *Proc Natl Acad Sci U S A* **101**: 6303-  
628 6308

629 **Guha S, Sarkar M, Ganguly P, Uddin MR, Mandal S, DasGupta M** (2016) Segregation of nod-  
630 containing and nod-deficient bradyrhizobia as endosymbionts of *Arachis hypogaea* and as  
631 endophytes of *Oryza sativa* in intercropped fields of Bengal Basin, India. *Environ Microbiol*  
632 **18**: 2575-2590

633 **Handberg K, Stougaard J** (1992) *Lotus japonicus*, an autogamous, diploid legume species for classical  
634 and molecular genetics. *Plant J* **2**: 487-496

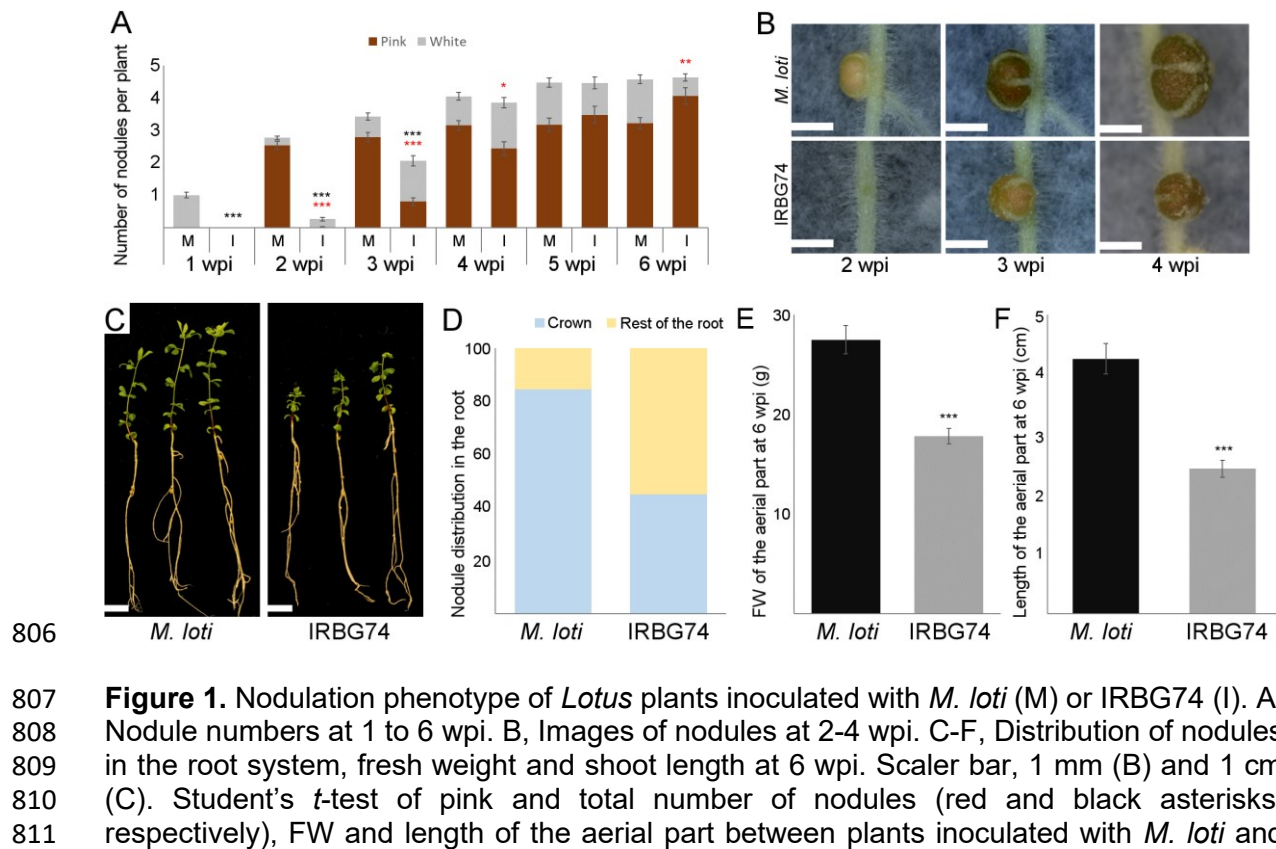
635 **Heckmann AB, Lombardo F, Miwa H, Perry JA, Bunnewell S, Parniske M, Wang TL, Downie JA**  
636 **(2006) Lotus japonicus** nodulation requires two GRAS domain regulators, one of which is  
637 functionally conserved in a non-legume. *Plant Physiol* **142**: 1739-1750

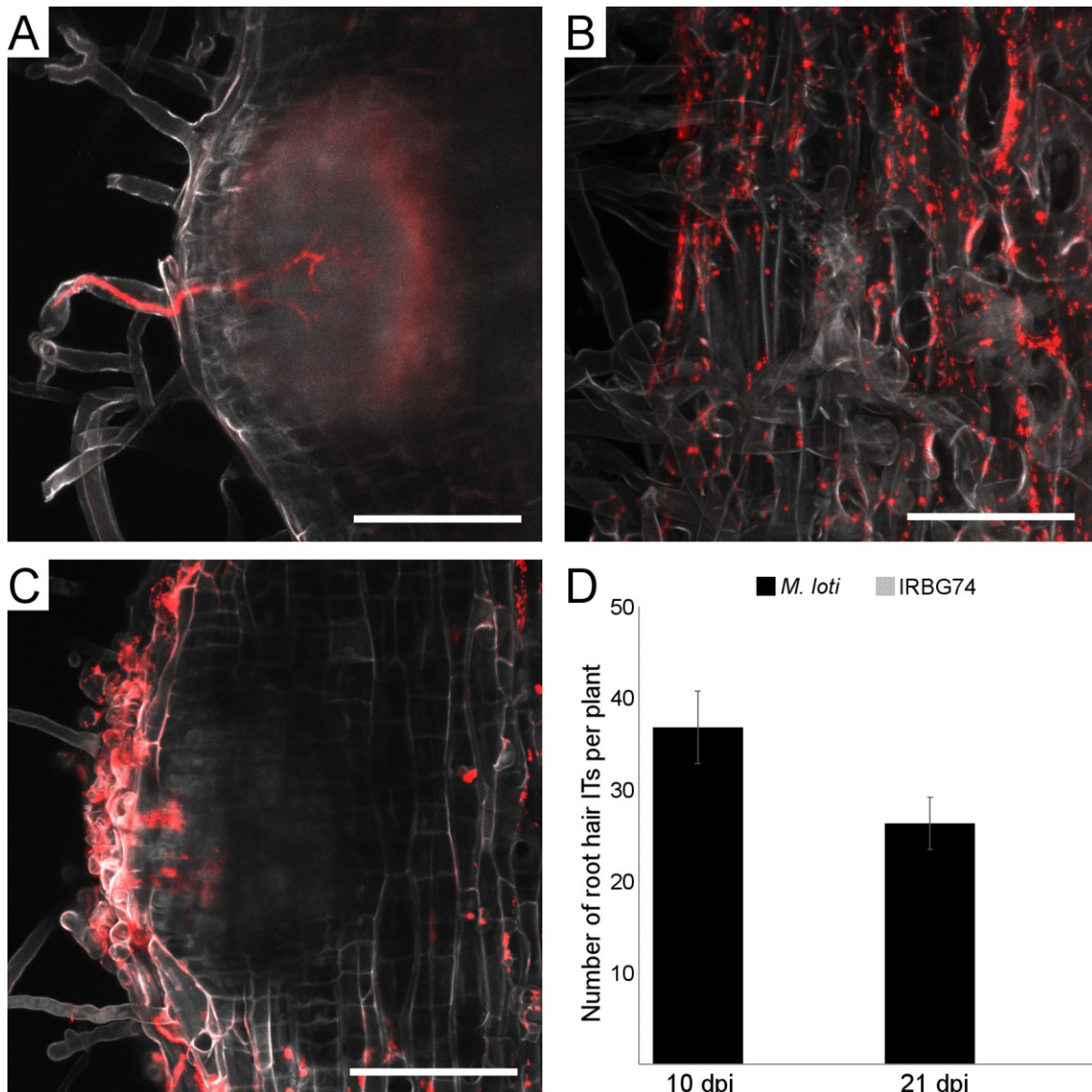
- 638 **Hossain MS, Liao J, James EK, Sato S, Tabata S, Jurkiewicz A, Madsen LH, Stougaard J, Ross L,**  
639 **Szczyglowski K** (2012) *Lotus japonicus* ARPC1 is required for rhizobial infection. *Plant Physiol*  
640 **160:** 917-928
- 641 **Hwang I, Sakakibara H** (2006) Cytokinin biosynthesis and perception. *Physiologia Plantarum* **126:**  
642 528-538
- 643 **Ibanez F, Fabra A** (2011) Rhizobial Nod factors are required for cortical cell division in the nodule  
644 morphogenetic programme of the Aeschynomeneae legume *Arachis*. *Plant Biol (Stuttg)* **13:**  
645 794-800
- 646 **Ibanez F, Wall L, Fabra A** (2017) Starting points in plant-bacteria nitrogen-fixing symbioses:  
647 intercellular invasion of the roots. *J Exp Bot* **68:** 1905-1918
- 648 **James EK, Sprent JI** (1999) Development of N<sub>2</sub>-fixing nodules on the wetland legume *Lotus*  
649 *uliginosus* exposed to conditions of flooding. *New Phytol* **142:** 219-231
- 650 **James EK, Sprent JI, Sutherland JM, McInroy SG, Minchin FR** (1992) The structure of nitrogen fixing  
651 root nodules on the aquatic Mimosoid legume *Neptunia plena*. *Annals of Botany* **69:** 173-  
652 180
- 653 **Kalo P, Gleason C, Edwards A, Marsh J, Mitra RM, Hirsch S, Jakab J, Sims S, Long SR, Rogers J, Kiss**  
654 **GB, Downie JA, Oldroyd GE** (2005) Nodulation signaling in legumes requires NSP2, a  
655 member of the GRAS family of transcriptional regulators. *Science* **308:** 1786-1789
- 656 **Kamal N, Mun T, Reid D, Lin J-S, Akyol TY, Sandal N, Asp T, Hirakawa H, Stougaard J, Mayer KFX,**  
657 **et al** (2020) A chromosome-scale *Lotus japonicus* Gifu genome assembly indicates that  
658 symbiotic islands are not general features of legume genomes. *bioRxiv* 2020.04.17.042473
- 659 **Karmakar K, Kundu A, Rizvi AZ, Dubois E, Severac D, Czernic P, Cartieaux F, DasGupta M** (2019)  
660 Transcriptomic Analysis With the Progress of Symbiosis in 'Crack-Entry' Legume *Arachis*  
661 hypogaea Highlights Its Contrast With 'Infection Thread' Adapted Legumes. *Mol Plant*  
662 *Microbe Interact* **32:** 271-285
- 663 **Kawaharada Y, James EK, Kelly S, Sandal N, Stougaard J** (2017) The Ethylene Responsive Factor  
664 Required for Nodulation 1 (ERN1) Transcription Factor Is Required for Infection-Thread  
665 Formation in *Lotus japonicus*. *Mol Plant Microbe Interact* **30:** 194-204
- 666 **Kawaharada Y, Kelly S, Nielsen MW, Hjuler CT, Gysel K, Muszynski A, Carlson RW, Thygesen MB,**  
667 **Sandal N, Asmussen MH, Vinther M, Andersen SU, Krusell L, Thirup S, Jensen KJ, Ronson**  
668 **CW, Blaise M, Radutoiu S, Stougaard J** (2015) Receptor-mediated exopolysaccharide  
669 perception controls bacterial infection. *Nature* **523:** 308-312
- 670 **Kelly SJ, Muszynski A, Kawaharada Y, Hubber AM, Sullivan JT, Sandal N, Carlson RW, Stougaard J,**  
671 **Ronson CW** (2013) Conditional requirement for exopolysaccharide in the Mesorhizobium-  
672 *Lotus* symbiosis. *Mol Plant Microbe Interact* **26:** 319-329
- 673 **Lace B, Ott T** (2018) Commonalities and Differences in Controlling Multipartite Intracellular  
674 Infections of Legume Roots by Symbiotic Microbes. *Plant Cell Physiol* **59:** 661-672
- 675 **Li X, Zheng Z, Kong X, Xu J, Qiu L, Sun J, Reid D, Jin H, Andersen SU, Oldroyd GED, Stougaard J,**  
676 **Downie JA, Xie F** (2019) Atypical Receptor Kinase RINRK1 Required for Rhizobial Infection  
677 But Not Nodule Development in *Lotus japonicus*. *Plant Physiol* **181:** 804-816
- 678 **Liang J, Klingl A, Lin YY, Boul E, Thomas-Oates J, Marin M** (2019) A subcompatible rhizobium strain  
679 reveals infection duality in *Lotus*. *J Exp Bot* **70:** 1903-1913
- 680 **Liu CW, Breakspear A, Stacey N, Findlay K, Nakashima J, Ramakrishnan K, Liu M, Xie F, Endre G, de**  
681 **Carvalho-Niebel F, Oldroyd GED, Udvardi MK, Fournier J, Murray JD** (2019) A protein  
682 complex required for polar growth of rhizobial infection threads. *Nat Commun* **10:** 2848
- 683 **Love MI, Huber W, Anders S** (2014) Moderated estimation of fold change and dispersion for RNA-  
684 seq data with DESeq2. *Genome Biol* **15:** 550

- 685 **Madsen EB, Madsen LH, Radutoiu S, Olbryt M, Rakwalska M, Szczyglowski K, Sato S, Kaneko T,**  
686 **Tabata S, Sandal N, Stougaard J** (2003) A receptor kinase gene of the LysM type is involved  
687 in legume perception of rhizobial signals. *Nature* **425**: 637-640
- 688 **Madsen LH, Tirichine L, Jurkiewicz A, Sullivan JT, Heckmann AB, Bek AS, Ronson CW, James EK,**  
689 **Stougaard J** (2010) The molecular network governing nodule organogenesis and infection  
690 in the model legume *Lotus japonicus*. *Nat Commun* **1**: 10
- 691 **Malolepszy A, Mun T, Sandal N, Gupta V, Dubin M, Urbanski D, Shah N, Bachmann A, Fukai E,**  
692 **Hirakawa H, Tabata S, Nadzieja M, Markmann K, Su J, Umehara Y, Soyano T, Miyahara A,**  
693 **Sato S, Hayashi M, Stougaard J, Andersen SU** (2016) The LORE1 insertion mutant resource.  
694 *Plant J* **88**: 306-317
- 695 **Marino D, Andrio E, Danchin EG, Oger E, Gucciardo S, Lambert A, Puppo A, Pauly N** (2011) A  
696 *Medicago truncatula* NADPH oxidase is involved in symbiotic nodule functioning. *New*  
697 *Phytol* **189**: 580-592
- 698 **Marsh JF, Rakocevic A, Mitra RM, Bocard L, Sun J, Eschstruth A, Long SR, Schultze M, Ratet P,**  
699 **Oldroyd GE** (2007) *Medicago truncatula* NIN is essential for rhizobial-independent nodule  
700 organogenesis induced by autoactive calcium/calmodulin-dependent protein kinase. *Plant*  
701 *Physiol* **144**: 324-335
- 702 **Miri M, Janakirama P, Held M, Ross L, Szczyglowski K** (2016) Into the Root: How Cytokinin Controls  
703 Rhizobial Infection. *Trends Plant Sci* **21**: 178-186
- 704 **Mitra S, Mukherjee A, Wiley-Kalil A, Das S, Owen H, Reddy PM, Ane JM, James EK, Gyaneshwar P**  
705 (2016) A rhamnose-deficient lipopolysaccharide mutant of *Rhizobium* sp. IRBG74 is  
706 defective in root colonization and beneficial interactions with its flooding-tolerant hosts  
707 *Sesbania cannabina* and wetland rice. *J Exp Bot* **67**: 5869-5884
- 708 **Montiel J, Arthikala M-K, Cárdenas L, Quinto C** (2016) Legume NADPH oxidases have crucial roles  
709 at different stages of nodulation. *International journal of molecular sciences* **17**: 680
- 710 **Montiel J, Nava N, Cardenas L, Sanchez-Lopez R, Arthikala MK, Santana O, Sanchez F, Quinto C**  
711 (2012) A *Phaseolus vulgaris* NADPH oxidase gene is required for root infection by Rhizobia.  
712 *Plant Cell Physiol* **53**: 1751-1767
- 713 **Morgante C, Castro S, Fabra A** (2007) Role of rhizobial EPS in the evasion of peanut defense  
714 response during the crack-entry infection process. *Soil Biology and Biochemistry* **39**: 1222-  
715 1225
- 716 **Mun T, Bachmann A, Gupta V, Stougaard J, Andersen SU** (2016) Lotus Base: An integrated  
717 information portal for the model legume *Lotus japonicus*. *Sci Rep* **6**: 39447
- 718 **Murakami E, Cheng J, Gysel K, Bozsoki Z, Kawaharada Y, Hjuler CT, Sorensen KK, Tao K, Kelly S,**  
719 **Venice F, Genre A, Thygesen MB, Jong N, Vinther M, Jensen DB, Jensen KJ, Blaise M,**  
720 **Madsen LH, Andersen KR, Stougaard J, Radutoiu S** (2018) Epidermal LysM receptor ensures  
721 robust symbiotic signalling in *Lotus japonicus*. *Elife* **7**
- 722 **Murray JD, Karas BJ, Sato S, Tabata S, Amyot L, Szczyglowski K** (2007) A cytokinin perception  
723 mutant colonized by *Rhizobium* in the absence of nodule organogenesis. *Science* **315**: 101-  
724 104
- 725 **Murray JD, Muni RR, Torres-Jerez I, Tang Y, Allen S, Andriankaja M, Li G, Laxmi A, Cheng X, Wen J,**  
726 **Vaughan D, Schultze M, Sun J, Charpentier M, Oldroyd G, Tadege M, Ratet P, Mysore KS,**  
727 **Chen R, Udvardi MK** (2011) Vapyrin, a gene essential for intracellular progression of  
728 arbuscular mycorrhizal symbiosis, is also essential for infection by rhizobia in the nodule  
729 symbiosis of *Medicago truncatula*. *Plant J* **65**: 244-252
- 730 **Nadzieja M, Stougaard J, Reid D** (2019) A Toolkit for High Resolution Imaging of Cell Division and  
731 Phytohormone Signaling in Legume Roots and Root Nodules. *Front Plant Sci* **10**: 1000

- 732 Oldroyd GE, Downie JA (2008) Coordinating nodule morphogenesis with rhizobial infection in  
733 legumes. *Annu Rev Plant Biol* **59**: 519-546
- 734 Patro R, Duggal G, Love MI, Irizarry RA, Kingsford C (2017) Salmon provides fast and bias-aware  
735 quantification of transcript expression. *Nat Methods* **14**: 417-419
- 736 Peleg-Grossman S, Volpin H, Levine A (2007) Root hair curling and Rhizobium infection in *Medicago*  
737 *truncatula* are mediated by phosphatidylinositide-regulated endocytosis and reactive  
738 oxygen species. *J Exp Bot* **58**: 1637-1649
- 739 Peng Z, Liu F, Wang L, Zhou H, Paudel D, Tan L, Maku J, Gallo M, Wang J (2017) Transcriptome  
740 profiles reveal gene regulation of peanut (*Arachis hypogaea* L.) nodulation. *Sci Rep* **7**: 40066
- 741 Poinsot V, Crook MB, Erdn S, Maillet F, Bascaules A, Ane JM (2016) New insights into Nod factor  
742 biosynthesis: Analyses of chitooligomers and lipo-chitooligomers of Rhizobium sp. IRBG74  
743 mutants. *Carbohydr Res* **434**: 83-93
- 744 Qiu L, Lin JS, Xu J, Sato S, Parniske M, Wang TL, Downie JA, Xie F (2015) SCARN a Novel Class of  
745 SCAR Protein That Is Required for Root-Hair Infection during Legume Nodulation. *PLoS*  
746 *Genet* **11**: e1005623
- 747 Radutoiu S, Madsen LH, Madsen EB, Felle HH, Umehara Y, Gronlund M, Sato S, Nakamura Y,  
748 Tabata S, Sandal N, Stougaard J (2003) Plant recognition of symbiotic bacteria requires two  
749 LysM receptor-like kinases. *Nature* **425**: 585-592
- 750 Ranga Rao V (1977) Effect of Root Temperature on the Infection Processes and Nodulation in Lotus  
751 and Stylosanthes. *J Exp Bot* **28**: 241-259
- 752 Reid D, Liu H, Kelly S, Kawaharada Y, Mun T, Andersen SU, Desbrosses G, Stougaard J (2018)  
753 Dynamics of Ethylene Production in Response to Compatible Nod Factor. *Plant Physiol* **176**:  
754 1764-1772
- 755 Reid D, Nadzieja M, Novak O, Heckmann AB, Sandal N, Stougaard J (2017) Cytokinin Biosynthesis  
756 Promotes Cortical Cell Responses during Nodule Development. *Plant Physiol* **175**: 361-375
- 757 Reid DE, Heckmann AB, Novak O, Kelly S, Stougaard J (2016) CYTOKININ  
758 OXIDASE/DEHYDROGENASE3 Maintains Cytokinin Homeostasis during Root and Nodule  
759 Development in *Lotus japonicus*. *Plant Physiol* **170**: 1060-1074
- 760 Schauer L, Roussis A, Stiller J, Stougaard J (1999) A plant regulator controlling development of  
761 symbiotic root nodules. *Nature* **402**: 191-195
- 762 Schindelin J, Arganda-Carreras I, Frise E, Kaynig V, Longair M, Pietzsch T, Preibisch S, Rueden C,  
763 Saalfeld S, Schmid B, Tinevez JY, White DJ, Hartenstein V, Eliceiri K, Tomancak P, Cardona  
764 A (2012) Fiji: an open-source platform for biological-image analysis. *Nat Methods* **9**: 676-  
765 682
- 766 Singh S, Katzer K, Lambert J, Cerri M, Parniske M (2014) CYCLOPS, a DNA-binding transcriptional  
767 activator, orchestrates symbiotic root nodule development. *Cell Host Microbe* **15**: 139-152
- 768 Sinharoy S, Torres-Jerez I, Bandyopadhyay K, Kereszt A, Pislariu CI, Nakashima J, Benedito VA,  
769 Kondorosi E, Udvardi MK (2013) The C2H2 transcription factor regulator of symbiosome  
770 differentiation represses transcription of the secretory pathway gene VAMP721a and  
771 promotes symbiosome development in *Medicago truncatula*. *Plant Cell* **25**: 3584-3601
- 772 Sprent JI (2007) Evolving ideas of legume evolution and diversity: a taxonomic perspective on the  
773 occurrence of nodulation. *New Phytol* **174**: 11-25
- 774 Sprent JI, Ardley J, James EK (2017) Biogeography of nodulated legumes and their nitrogen-fixing  
775 symbionts. *New Phytol* **215**: 40-56
- 776 Subba-Rao NS, Mateos PF, Baker D, Pankratz HS, Palma J, Dazzo B, Sprent JI (1995) The unique  
777 root-nodule symbiosis between Rhizobium and the aquatic legume, *Neptunia natans* (L. f.)  
778 Druce. *Planta* **196**: 311-320

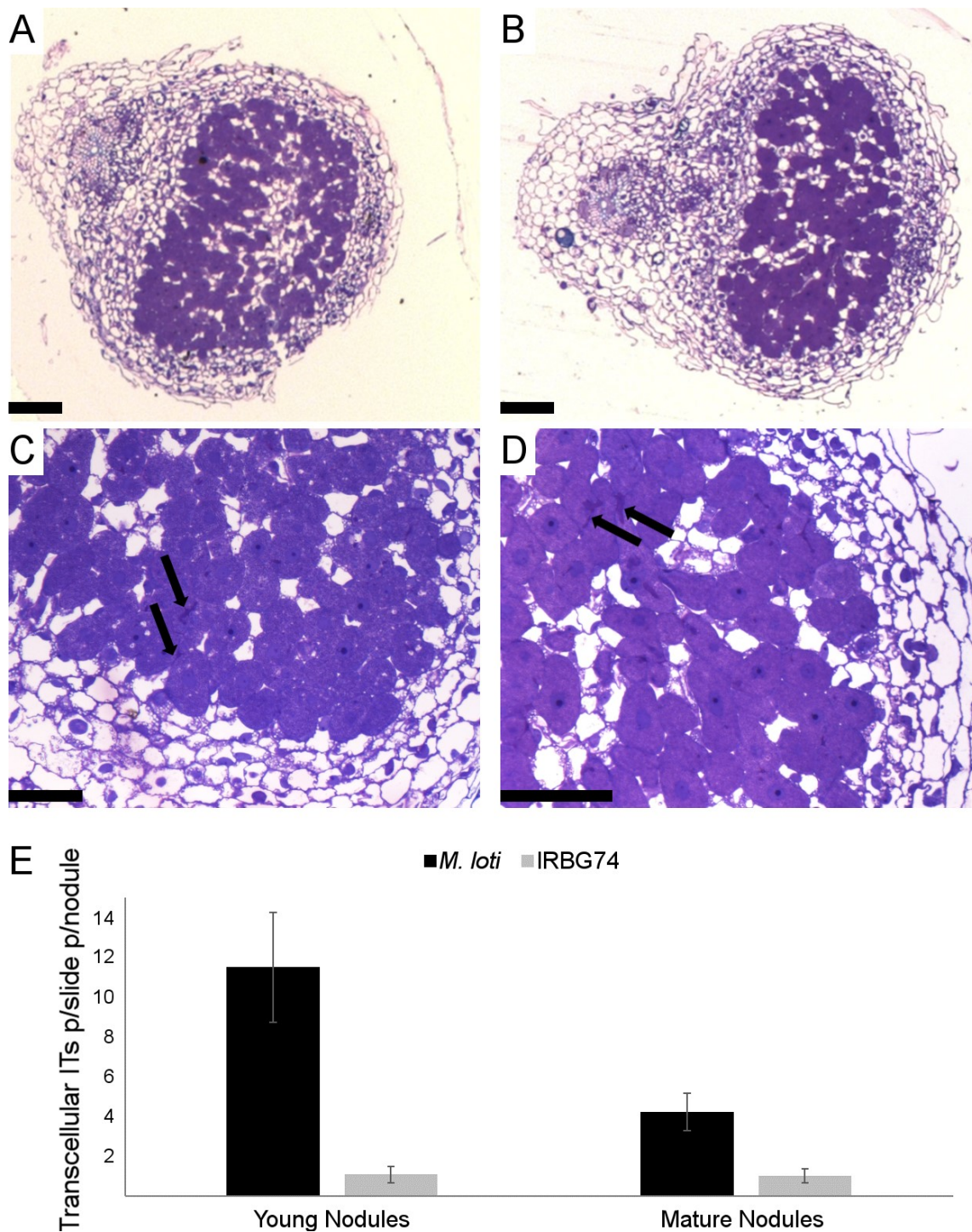
- 779 **Takei K, Yamaya T, Sakakibara H** (2004) Arabidopsis CYP735A1 and CYP735A2 encode cytokinin  
780 hydroxylases that catalyze the biosynthesis of trans-Zeatin. *J Biol Chem* **279**: 41866-41872  
781 **Urbanski DF, Malolepszy A, Stougaard J, Andersen SU** (2012) Genome-wide LORE1 retrotransposon  
782 mutagenesis and high-throughput insertion detection in *Lotus japonicus*. *Plant J* **69**: 731-  
783 741  
784 **Vega-Hernandez MC, Perez-Galdona R, Dazzo FB, Jarabo-Lorenzo A, Alfayate MC, Leon-Barrios M**  
785 (2001) Novel infection process in the indeterminate root nodule symbiosis between  
786 *Chamaecytisus proliferus* (tagasaste) and *Bradyrhizobium* sp. *New Phytol* **150**: 707-721  
787 **Xie F, Murray JD, Kim J, Heckmann AB, Edwards A, Oldroyd GE, Downie JA** (2012) Legume pectate  
788 lyase required for root infection by rhizobia. *Proc Natl Acad Sci U S A* **109**: 633-638  
789 **Yano K, Shibata S, Chen WL, Sato S, Kaneko T, Jurkiewicz A, Sandal N, Banba M, Imaizumi-Anraku**  
790 **H, Kojima T, Ohtomo R, Szczyglowski K, Stougaard J, Tabata S, Hayashi M, Kouchi H, Umehara Y** (2009) CERBERUS, a novel U-box protein containing WD-40 repeats, is required  
791 for formation of the infection thread and nodule development in the legume-Rhizobium  
792 symbiosis. *Plant J* **60**: 168-180  
793  
794 **Yano K, Yoshida S, Muller J, Singh S, Banba M, Vickers K, Markmann K, White C, Schuller B, Sato**  
795 **S, Asamizu E, Tabata S, Murooka Y, Perry J, Wang TL, Kawaguchi M, Imaizumi-Anraku H, Hayashi M, Parniske M** (2008) CYCLOPS, a mediator of symbiotic intracellular  
796 accommodation. *Proc Natl Acad Sci U S A* **105**: 20540-20545  
797  
798 **Yokota K, Fukai E, Madsen LH, Jurkiewicz A, Rueda P, Radutoiu S, Held M, Hossain MS, Szczyglowski K, Morieri G, Oldroyd GE, Downie JA, Nielsen MW, Rusek AM, Sato S, Tabata S, James EK, Oyaizu H, Sandal N, Stougaard J** (2009) Rearrangement of actin cytoskeleton  
800 mediates invasion of *Lotus japonicus* roots by *Mesorhizobium loti*. *Plant Cell* **21**: 267-284  
801  
802 **Zhao CZ, Huang J, Gyaneshwar P, Zhao D** (2017) Rhizobium sp. IRBG74 Alters Arabidopsis Root  
803 Development by Affecting Auxin Signaling. *Front Microbiol* **8**: 2556  
804  
805





815

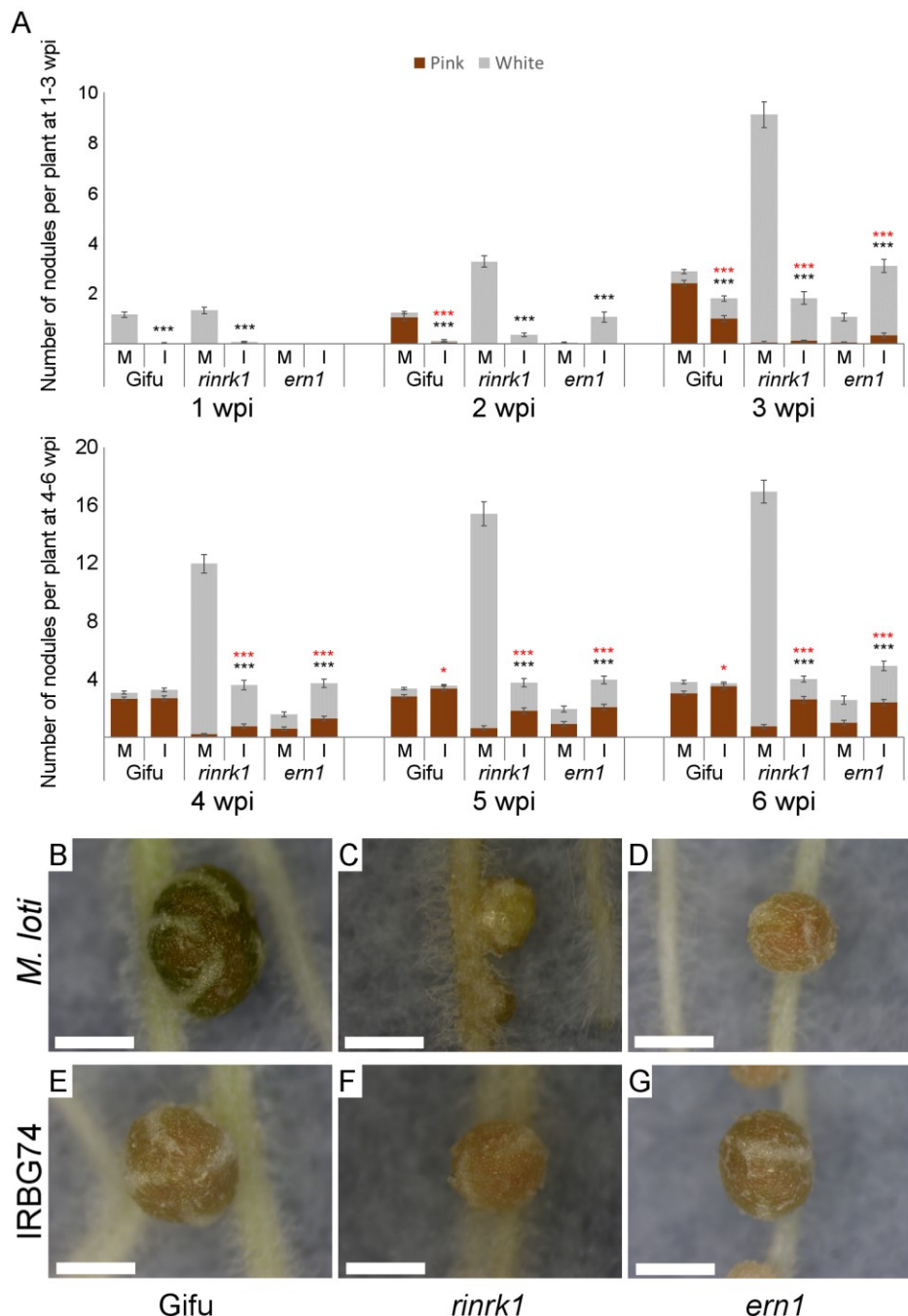
816 **Figure 2.** Intracellular and intercellular rhizobial infection of *Lotus* roots. Confocal  
817 microscopy images of *Lotus* roots at 1 wpi (A and B) and 2 wpi (C) with *M. loti* -DsRed (A)  
818 or IRBG74-DsRed (B and C). Scale bar, 50  $\mu$ m. D, number of root hair ITs in *Lotus* plants  
819 at 10 dpi and 21 dpi with *M. loti* -DsRed or IRBG74-DsRed ( $n \geq 15$ ). Error bars mean SEM.  
820



821

822 **Figure 3.** Histology of *Lotus* nodules colonized by *M. loti* or IRBG74. Sections from young  
823 nodules of *Lotus* inoculated with *M. loti* (A and C) or IRBG74 (B and D) were stained with  
824 toluidine blue to evaluate rhizobial occupancy in the nodule cells. Transcellular infection  
825 threads are indicated with arrows. Scale bar, 100  $\mu$ m (A and B) and 50  $\mu$ m (C and D). E,  
826 number of transcellular ITs in 7 slides from 7 different young (Y) and mature (M) nodules.  
827 Error bars mean SEM.

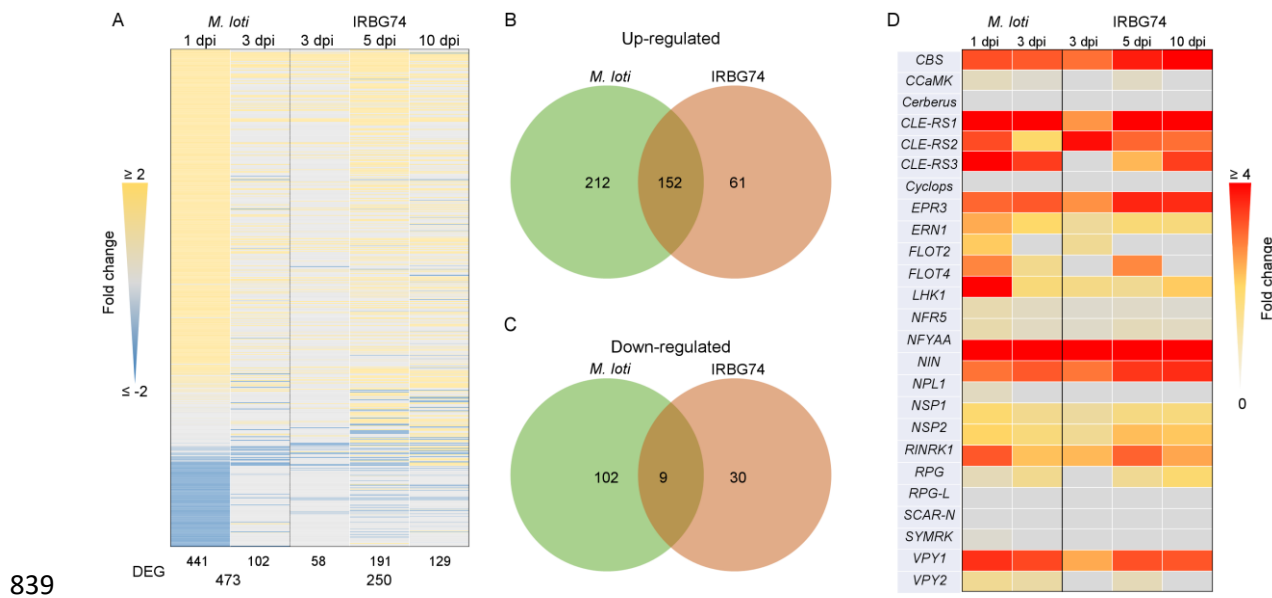
828



829

830 **Figure 4.** Nodulation phenotype of *rinrk1* and *ern1* mutants. Nodulation kinetics from 1-6  
831 wpi (A) with *M. loti* (M) or *IRBG74* (I) in *rinrk1* and *ern1*. Error bars mean SEM. Student's *t*-  
832 test of pink and total number of nodules (red and black asterisks, respectively) between  
833 plants inoculated with *M. loti* or *IRBG74* in the same genetic background. P-values < 0.05  
834 and 0.001 are marked with one or three asterisks, respectively. n = *Gifu* 59 (M), 69 (I); *rinrk1*  
835 49 (M), 55 (I); *ern1* 48 (M), 59 (I). Representative images of nodules at 4 wpi with *IRBG74*  
836 (E, F and G) or *M. loti* (B, C and D) from *Gifu* (B and E), *rinrk1* (C and F) and *ern1* (D and  
837 G). Scale bar 1 cm (G) and 1 mm (H-J).

838



840 **Figure 5.** Comparison of the transcriptomic profile of *Lotus* roots during intracellular and  
841 intercellular rhizobial infection. A, heat-map expression of DEG (LOG2FC  $\geq 2$  and a P-adjust  
842  $< 0.5$ ) in after *M. loti* or IRBG74 inoculation. B and C, Ven diagrams with total number (*M.*  
843 *loti*: 1 and 3dpi; IRBG74: 3, 5 and 10 dpi) of the up/down regulated DEG during intracellular  
844 (*M. loti*) and intercellular (IRBG74) colonization. D, heat-map expression of known SYM  
845 genes significantly (P-adjust  $< 0.5$ ) induced after rhizobial perception.

846



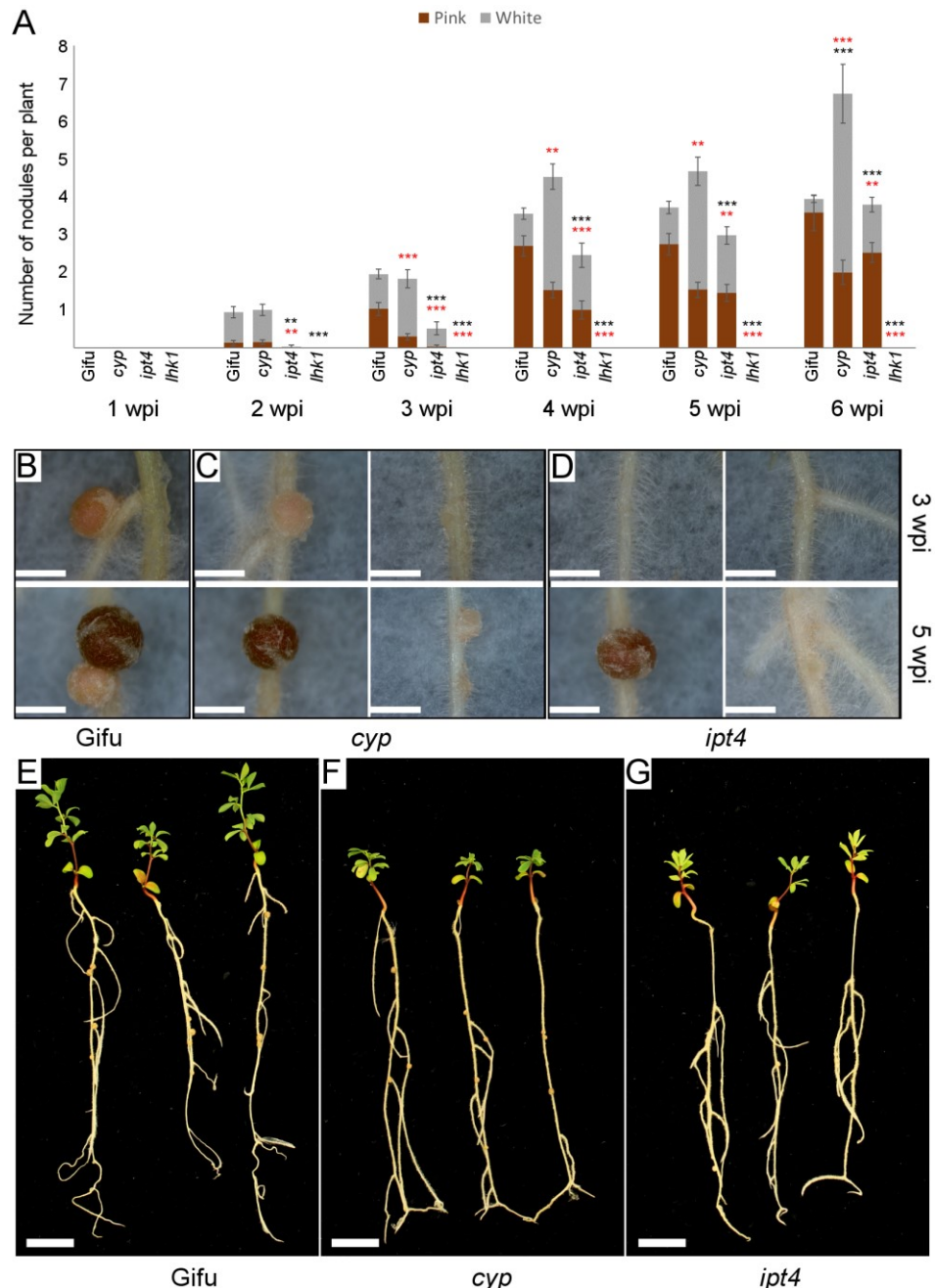
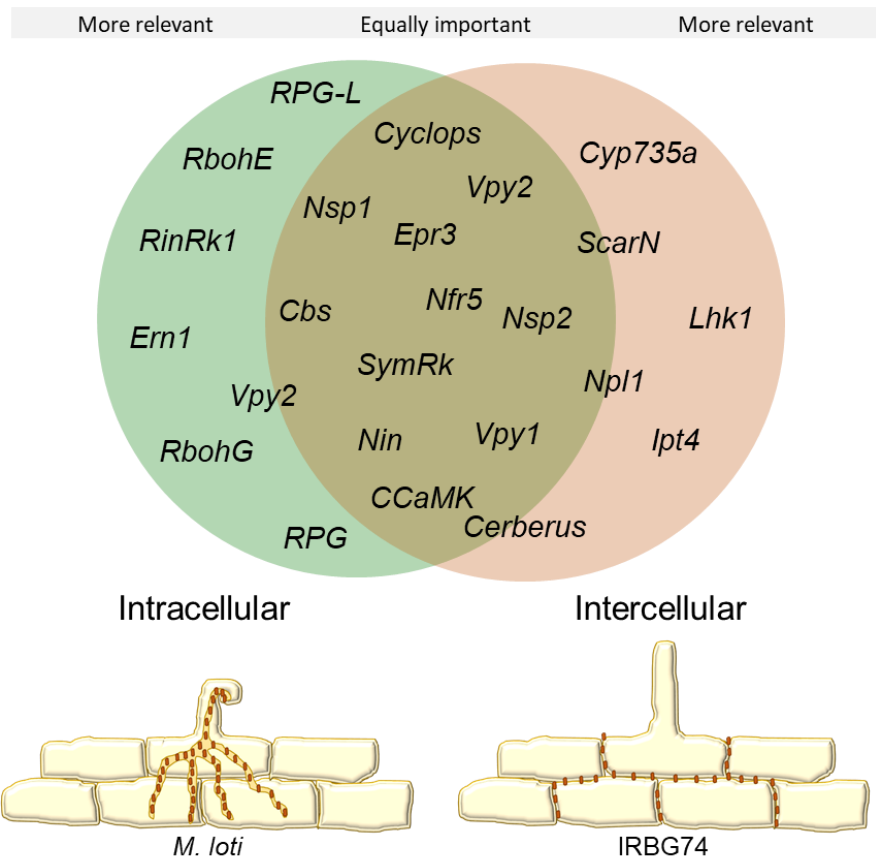


**Figure 7.** Symbiotic phenotype of *Lotus* mutants affected in cytokinin-related genes. A, nodulation kinetics of *cyp735a*, *ipt4* and *lhk1* plants from 1 to 6 wpi with IRBG74. Error bars mean SEM. Student's *t*-test analyses of pink nodules and total number of nodules (red and black asterisks, respectively) between w. t. and mutant plants inoculated with IRBG74. *P*-values < 0.01 and 0.001 are marked with two or three asterisks, respectively. *n* = 49 (Gifu), 86 (*cyp735a*), 53 (*ipt4*), 55 (*lhk1*). Phenotype of nodules developed in w. t. (B), *cyp735a* (C) and *ipt4* (D) plants at 3 (upper panel) and 5 wpi (lower panel) with IRBG74. Representative images of w. t. (E), *cyp735a* (F) and *ipt4* (G) plants at 6 wpi with IRBG74. Scale bar, 1 mm (B-D) and 1 cm (E-G).

863



864

865 **Figure 8.** Comparative model of gene requirements in the intracellular and intercellular  
866 symbiotic program in *Lotus*. *Lotus* recruits a core of essential genes for the root nodule  
867 symbiosis, regardless the type of infection mechanism employed by rhizobia. Nonetheless,  
868 certain players are particularly more relevant depending on the mode of colonisation.  
869 Intercellular infection in *Lotus* appears to be more sensitive to the absence of certain  
870 cytokinin-related genes.

871